DOI: 10.1002/anie.201307650

Metal–Organic Frameworks

A Cationic Metal–Organic Framework Consisting of Nanoscale Cages: Capture, Separation, and Luminescent Probing of $Cr_2O_7^{2-}$ through a Single-Crystal to Single-Crystal Process**

*Xinxiong Li, Hongyan Xu, Fanzhen Kong, and Ruihu Wang**

With the development of modern industry, heavy-metal contamination has become a more and more severe problem. Among common heavy-metal pollutants, hexavalent chromium [Cr^{VI}] has been a focus of concern because it causes serious damage to human health and the environment.[1] Cr^{VI} has been widely used in the field of chromium plating, metallurgy, pigment manufacturing, leather tanning, and wood preservation.[2] The capture and separation of Cr^{VI} from industrial waste water is extremely important. Although adsorbents,[3] resins,[4] and membranes[5] have been introduced to remove Cr^{VI} and other pollutants, their inherent drawbacks, such as poor selectivity and slow process kinetics, limit their further development and application. Therefore, the exploration of new materials for the efficient capture and separation of Cr^{VI} is highly important.

As an emerging class of porous materials, metal–organic frameworks (MOFs) have recently attracted considerable attention owing to their high surface area, uniform pore size, controllable structures, and readily tailorable functions.[6] Cationic MOFs are an appealing subclass and can be constructed by using neutral nitrogen-containing organic ligands and metal ions. The charge-balancing anions usually occupy the framework voids and are sometimes just weakly coordinated or even uncoordinated to the metal centers, potentially allowing the capture and separation of anions through anion exchange. Recently, a few cationic MOFs have been used for exchange and removal of heavy-metal pollutant anions, such as ReO_4^-, CrO_4^{2-}, and TcO_4^-,[7] but there has been no report of $Cr_2O_7^{2-}$ anion exchange in MOFs despite the powerful carcinogenicity and extensive application of this species. Herein, we report an unprecedented 3D cationic MOF consisting of nanoscale cages composed of $[Ag_2(btr)_2]\cdot 2ClO_4\cdot 3H_2O$ ($ABT\cdot 2ClO_4$; (btr = 4,4′-bis(1,2,4-triazole)) , which shows fast exchange, high trapping capacity, and good selectivity for the capture and separation of $Cr_2O_7^{2-}$ in water. Interestingly, the exchange of $Cr_2O_7^{2-}$ in $ABT\cdot 2ClO_4$ was performed through a single-crystal to single-crystal (SC–SC) process.

Colorless crystals of $ABT\cdot 2ClO_4$ were obtained by slow evaporation of a solution of $AgClO_4$ and btr in water and acetonitrile. Single-crystal X-ray diffraction analysis revealed that $ABT\cdot 2ClO_4$ crystallizes in the cubic space group $Fd\bar{3}c$. As shown in Figure 1, two independent Ag^I ions adopt a distorted tetrahedral coordination geometry and are coordinated by four nitrogen atoms from different btr ligands, Ag–N bond lengths range from 2.237(5) Å to 2.417(6) Å. Two crystallographically independent btr molecules act as tetradentate ligands to bridge four Ag^I ions (Scheme S1 in the Supporting Information); the two triazolyl rings in btr are nearly perpendicular to each other, and the twisting angles between them are 85.540(3) and 74.599(3)°, respectively. A prominent structural feature of $ABT\cdot 2ClO_4$ is the presence of distorted octahedral and tetrahedral cages. The octahedral cage is made up of twelve Ag^I ions and twelve btr ligands (Figure 2a and S1); the overall edge length is about 2.0 nm and the inner diameter and calculated pore volume based on the van der Waals surfaces are about 4.18 Å and 305.9 $Å^3$, respectively. Each octahedral cage has eight trigonal windows formed by three Ag^I ions and three btr ligands, and the aperture of these windows is about 4.0 Å. The tetrahedral cage consists of eight Ag^I ions and eight btr ligands and its edge length is about 1.0 nm (Figure 2b and S1). Worthy of mention is further assembly of these cages. Each octahedral cage is connected to

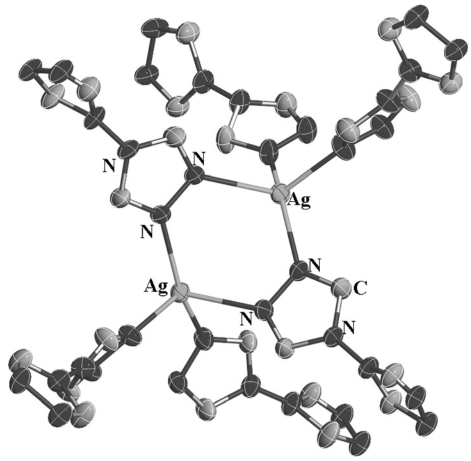

Figure 1. Crystal structure showing the coordination environments of the Ag^I ions in $ABT\cdot 2ClO_4$ with thermal ellipsoids set at 50% probability.

---

[*] Dr. X. X. Li, H. Y. Xu, F. Z. Kong, Prof. Dr. R. H. Wang
State Key Laboratory of Structural Chemistry
Fujian Institute of Research on the Structure of Matter
Chinese Academy of Sciences, Fuzhou, Fujian 350002 (China)
E-mail: ruihu@fjirsm.ac.cn

[**] This work was financially supported by 973 Program (2010CB933501, 2011CBA00502), Natural Science Foundation of China (21273239) and "One Hundred Talent Project" from Chinese Academy of Sciences.

Supporting information for this article is available on the WWW under http://dx.doi.org/10.1002/anie.201307650.

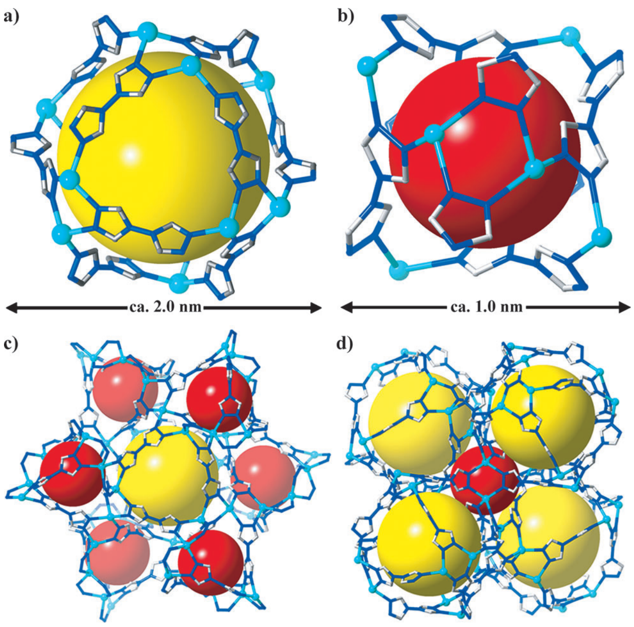

Figure 2. Ball and stick representation of the octahedral (a) tetrahedral (b) cages of ABT·2 ClO_4; c) The linking mode of an octahedral cage with six tetrahedral cages; d) The linking mode of a tetrahedral cage with four octahedral cages. The large spheres indicate the sizes of the voids. N blue, C white, Ag small light-blue spheres.

six tetrahedral cages through the sharing of two Ag^I ions and two btr ligands (Figure 2 c and S2), while every tetrahedral cage shares Ag^I ions and btr ligands with four octahedral cages (Figure 2 d and S2). The linking of the two types of cage results in the formation of a 3D cationic framework (Figure 3 and S3). The framework possesses 1D channels with a diameter of about 7.8 Å along [1 1 1] direction, which should be accessible to anion exchange. Although a large number of cationic MOFs have been reported,[8] cationic MOFs constructed from nanoscale coordination cages are very rare.[9] PLATON calculation showed that the total empty volume of the cationic framework is 65 531 Å^3, corresponding to 52.8 % of the total crystal volume (124 045 Å^3). The cavities and channels were filled with highly disordered ClO_4^- anions and lattice water molecules that cannot be completely mapped by single-crystal X-ray diffraction, which is often observed in high-symmetry structures.[10]

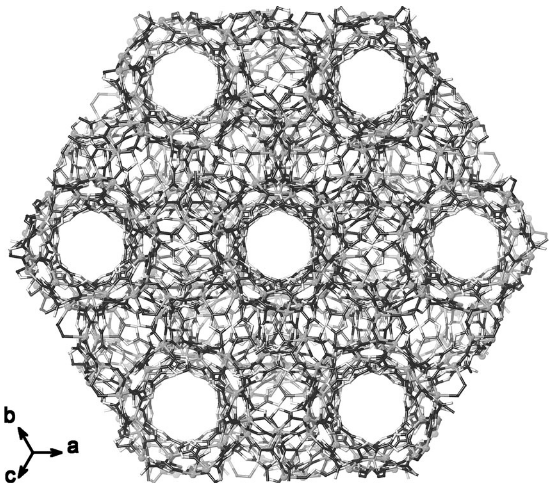

Figure 3. 3D cationic framework with 1D channels along [1 1 1] direction in ABT·2 ClO_4.

Crystalline ABT·2 ClO_4 is stable in water and common organic solvents. The good agreement between the experimental pattern and the simulated pattern for the powder X-ray diffraction (PXRD) indicates phase purity of ABT·2 ClO_4 (Figure 4). PXRD also indicated that ABT·2 ClO_4 can keep its crystallinity after immersion in aqueous solutions of $HClO_4$ and NaOH with pH values ranging from zero to ten for 24 h (Figure S4). Thermogravimetric analysis (TGA; Figure S5) of ABT·2 ClO_4 showed a weight loss of 7.10 % over the temperature range 30–220 °C, corresponding to the removal of lattice water molecules (calcd 7.29 %). Above 220 °C, framework collapse was observed, which is further supported by variable-temperature PXRD (Figure S6). In the IR spectrum of ABT·2 ClO_4 (Figure S7), characteristic vibration bands arising from charge-balancing ClO_4^- were located at 1050–1150 cm^{-1},[11] which is consistent with the single-crystal structural analysis.

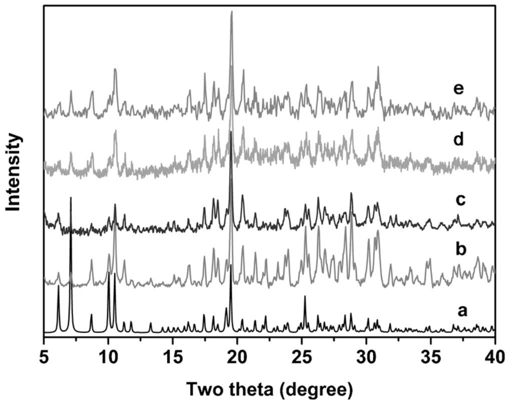

Figure 4. PXRD patterns for: a) simulated ABT·2 ClO_4; b) as-synthesized ABT·2 ClO_4; c) ABT·2 ClO_4 immersed in equimolar aqueous $K_2Cr_2O_7$ solution for 48 h; d) ABT·2 ClO_4 immersed in aqueous solution of excess $K_2Cr_2O_7$; e) ABT·2 ClO_4 immersed in aqueous solution of equimolar $K_2Cr_2O_7$, with double the molar amount of BF_4^-, $CF_3SO_3^-$, and NO_3^- ions.

Given that a great deal of ClO_4^- is located in the voids of the framework of ABT·2 ClO_4 and that enough large channels are available for anion access, anion exchange experiments were performed using $Cr_2O_7^{2-}$ as a model. The exchange process was monitored by UV/Vis spectroscopy at intervals based on the intensity variation of the maximum adsorption peak of $Cr_2O_7^{2-}$ in solution (257 nm).[12] As shown in Figure 5, when crystals of ABT·2 ClO_4 (0.05 mmol) were immersed in a 20 mL aqueous solution of equimolar $K_2Cr_2O_7$, the $Cr_2O_7^{2-}$ concentration in solution decreased by 37 % and 60 % after 1 h and 3 h, respectively, results corresponding to capture capacities of 0.37 and 0.60 mol mol^{-1}, respectively. Subsequently, a slow decrease in $Cr_2O_7^{2-}$ concentration was observed, and there were no obvious changes in anion concentration and solution color between 24 h and 48 h

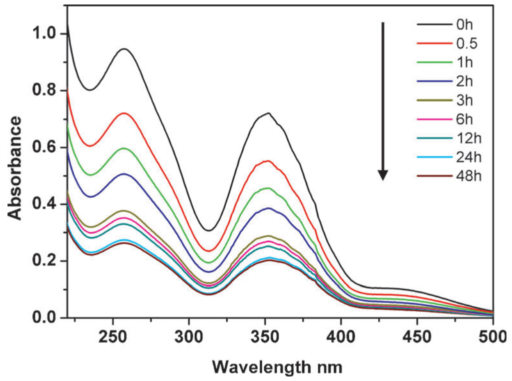

Figure 5. UV/Vis spectra of aqueous $K_2Cr_2O_7$ solution during exchange with equimolar ABT·2 ClO_4.

(Figure 5 and S8). The overall capacity of ABT·2 ClO_4 to capture $Cr_2O_7^{2-}$ is 0.73 mol mol^{-1} after 48 h, which is consistent with inductively coupled plasma atomic emission spectroscopy (ICP–AES) analysis (0.71 mol mol−1). To date, anion exchange of $Cr_2O_7^{2-}$ by cationic crystalline materials has rarely been reported. The only example is a layered inorganic lead fluoride material,[12] which exhibited only a 0.52 mol mol^{-1} exchange capacity for $Cr_2O_7^{2-}$ in a 50% excess concentration of aqueous $K_2Cr_2O_7$ solution after 7 days; moreover, some concomitant decomposition to PbF_2 or $PbCr_2O_7$ was found. By comparison, ABT·2 ClO_4 has a superior performance for $Cr_2O_7^{2-}$ capture with fast exchange and high capacity.

When using double the molar amount of ABT·2 ClO_4 with respect to $Cr_2O_7^{2-}$ under the same conditions, 66% and 90% of $Cr_2O_7^{2-}$ were exchanged after 0.5 h and 6 h, respectively (Figure S9). The UV/Vis adsorption intensity of $Cr_2O_7^{2-}$ remained almost constant after 6 h, thus indicating completion of the exchange process. During exchange, the solution changed from yellow to colorless (Figure S10). The total adsorption capacity after 48 h as defined by UV/Vis spectroscopy and ICP–AES analysis are 0.93 and 0.92 mol mol^{-1}, respectively.

The $Cr_2O_7^{2-}$ capture ability was further investigated in more dilute aqueous solutions. As shown in Figure S11, when excess ABT·2 ClO_4 was placed in a 14.7 ppm aqueous solution of $K_2Cr_2O_7$, the crystals changed from colorless to yellow after 48 h. UV/Vis spectroscopy showed that the characteristic adsorption peak of $Cr_2O_7^{2-}$ in solution vanished completely (Figure S12), and ICP–AES analysis showed that the concentration of remnant $Cr_2O_7^{2-}$ was 0.09 ppm, thus suggesting almost complete capture of $Cr_2O_7^{2-}$ (99.4%) by ABT·2 ClO_4. These results imply that ABT·2 ClO_4 is a promising material for the removal of low-concentration $Cr_2O_7^{2-}$ from waste water.

To further explore whether the ClO_4^- in the framework of ABT·2 ClO_4 can be completely exchanged, as-synthesized crystals were immersed in an aqueous solution containing excess $K_2Cr_2O_7$. After anion exchange, the resultant orange-yellow crystals (denoted as ABT·Cr_2O_7) were collected by filtration, rinsed with deionized water, and dried in air. Interestingly, the apparent morphology of the crystals showed no obvious change (Figure S13). ICP–AES analysis of ABT·Cr_2O_7 revealed that the molar ratio of Ag to Cr is 1:1, suggesting that ClO_4^- was fully exchanged by $Cr_2O_7^{2-}$. The PXRD pattern of ABT·Cr_2O_7 was identical with that of ABT·2 ClO_4 (Figure 4). In the IR spectrum of ABT·Cr_2O_7 (Figure S7), the emergence of the characteristic adsorption band arising from $Cr_2O_7^{2-}$ at about 771 cm^{-1}[13] and the concomitant disappearance of the broad band arising from ClO_4^- at 1090 cm^{-1} were observed, thus indicating that $Cr_2O_7^{2-}$ from the solution entered the framework of ABT·2 ClO_4 by complete exchange with ClO_4^-. TGA analysis showed that ABT·Cr_2O_7 was stable up to 210 °C, a slightly lower temperature than that measured for ABT·2 ClO_4 (Figure S5). In contrast to ABT·2ClO_4, a sharp drop was observed in the TGA curve of ABT·Cr_2O_7 after 210 °C, which was attributed to the drastic decomposition of ABT·Cr_2O_7. To further confirm the framework stability and the anion exchange process, a crystal of ABT·Cr_2O_7 was subject to single-crystal X-ray diffraction. As shown in Figures S14 and S15, the whole cationic framework is still intact after anion exchange; $Cr_2O_7^{2-}$ fills the voids in the framework to balance the charge. These observations indicate that anion exchange took place through a SC–SC process. To our knowledge, SC–SC transformation of heavy metal pollutant anions has not been explored, although a few examples of solid–solid exchange have been reported.[7] Moreover, ABT·Cr_2O_7 is the first reported example of a 3D MOF able to take up $Cr_2O_7^{2-}$ counter anions.

In comparison with anion exchange, anion selectivity may be more important and challenging. Selective exchange experiments were examined for mixtures of anions. When the crystals of 0.05 mmol ABT·2 ClO_4 were immersed in a 20 mL aqueous solution containing 0.1 mmol BF_4^-, 0.1 mmol $CF_3SO_3^-$, 0.1 mmol NO_3^- and 0.05 mmol $Cr_2O_7^{2-}$ for 24 h, the crystals gradually turned yellow. In the IR spectrum of the resultant crystals (Figure S16), only the characteristic band arising from $Cr_2O_7^{2-}$ was found; no characteristic adsorption bands arising from NO_3^- (1385 cm^{-1}), $CF_3SO_3^-$ (1265 cm^{-1}), or BF_4^- (1080–1030 cm^{-1}) were observed,[11,14] thus suggesting good selectivity for $Cr_2O_7^{2-}$ over NO_3^-, $CF_3SO_3^-$, and BF_4^- ions. The selectivity of ABT·2 ClO_4 may be attributed to a stronger interaction of $Cr_2O_7^{2-}$ with the cationic framework than NO_3^-, $CF_3SO_3^-$, and BF_4^- ions.[8c]

The effect of anion exchange on luminescence was also explored. As shown in Figure 6, ABT·2 ClO_4 emitted a bluish-violet light under UV irradiation, whereas the ABT·Cr_2O_7 emission is almost invisible to naked eye. The solid-state emission spectrum of ABT·2 ClO_4 at room temperature displays a broad emission band centered at 450 nm upon excitation at 345 nm, a value in agreement with the emission observed under UV irradiation. The emission may be attributed to ligand-to-metal charge transfer (LMCT) transition.[15] However, the luminescent emission was largely suppressed after the exchange of ClO_4^- by $Cr_2O_7^{2-}$. The disappearance of the luminescent emission in ABT·Cr_2O_7 is probably because the electron-transfer transitions of $Cr_2O_7^{2-}$ decrease the energy transfer from the btr ligand to Ag^I.[7b] ABT·2 ClO_4 may thus be considered a luminescent probe for

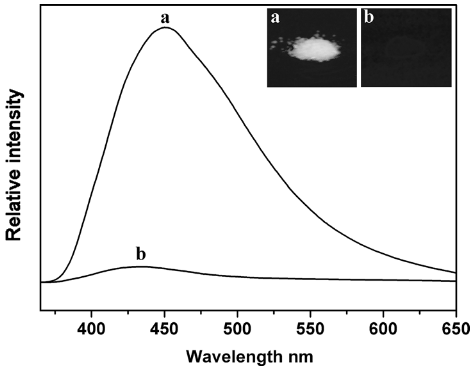

Figure 6. Room-temperature solid-state emission spectra upon excitation at 345 nm for a) ABT·2 ClO_4 and b) ABT·Cr_2O_7. Insert: fluorescent images under UV irradiation for a) ABT·2 ClO_4 and b) ABT·Cr_2O_7.

$Cr_2O_7^{2-}$, an application that has not hitherto been reported for MOFs.

In conclusion, an unprecedented 3D cationic MOF consisting of distorted octahedral and tetrahedral cages has been successfully prepared. Anion exchange studies showed that the complex sets a record for fast capture and removal of $Cr_2O_7^{2-}$, moreover, $Cr_2O_7^{2-}$ exchange took place through SC–SC transformation. The use of MOFs that are able to take up pollutant anions could thus prove an effective strategy for dealing with pollutants of this type that are difficult to remove through established methods. ABT·2 ClO_4 exhibits a bluish violet luminescence that is distinctly quenched upon $Cr_2O_7^{2-}$ exchange; ABT·2ClO_4 may thus be used as a luminescent probe for $Cr_2O_7^{2-}$. This work not only enriches the structural diversity of MOFs, but also widens the application of MOFs to the capture, enrichment, and luminescence-based detection of $Cr_2O_7^{2-}$.

Experimental Section

Crystal data for ABT·2 ClO_4: $C_8H_{14}N_{12}O_{11}Cl_2Ag_2$, Cubic, $Fd\bar{3}c$, $a = 49.8724(6)$ Å, $V = 124\,045(3)$ Å^3, $Z = 192$, $\rho = 1.904\ \mathrm{g\,cm^{-3}}$, $F(000) = 69\,504$, GOF = 1.039, $R_1 = 0.0618$, $wR_2 = 0.1752$. Crystal data for ABT·Cr_2O_7: $C_8H_{10}N_{12}O_8Cr_2Ag_2$, Cubic, $Fd\bar{3}c$, $a = 49.869(2)$ Å, $V = 124\,022(9)$ Å^3, $Z = 192$, $\rho = 1.856\ \mathrm{g\,cm^{-3}}$, $F(000) = 66\,816$, GOF = 1.237, $R_1 = 0.0604$, $wR_2 = 0.1517$. Full experimental details are given in the Supporting Information. CCDC 927379 and 939626 contain the supplementary crystallographic data for this paper. These data can be obtained free of charge from The Cambridge Crystallographic Data Centre via www.ccdc.cam.ac.uk/data_request/cif.

Received: August 30, 2013

Keywords: anion exchange · dichromate · luminescence · metal–organic frameworks · single-crystal to single-crystal transformation

---

[1] a) M. Costa, C. B. Klein, *Crit. Rev. Toxicol.* **2006**, *36*, 155–163; b) S. Kaneko, M. Ogawa, *Appl. Clay Sci.* **2013**, *28*, 109–158; c) E. Darakas, V. Tsiridis, M. Petala, A. Kungolos, *J. Environ. Sci. Health Part A* **2013**, *48*, 1390–1398.

[2] a) L. Khezami, R. J. Capart, *J. Hazard. Mater.* **2005**, *123*, 223–231; b) B. Dhal, H. N. Thatoi, N. N. Das, B. D. Pandey, *J. Hazard. Mater.* **2013**, *250*, 272–291.

[3] a) L. M. Blaney, S. Cinar, A. K. SenGupta, *Water Res.* **2007**, *41*, 1603–1613; b) L. L. Li, L. L. Fan, M. Sun, H. M. Qiu, X. J. Li, H. M. Duan, C. N. Luo, *Colloids Surf. B* **2013**, *107*, 76–83.

[4] a) S. V. Prasanna, P. V. Kamath, *Solid State Sci.* **2008**, *10*, 260–266; b) N. V. Nguyen, J. Jeong, J. C. Lee, *J. Chem. Technol. Biotechnol.* **2013**, *88*, 1014–1022.

[5] a) A. K. Chakravarti, A. K. Chowdhury, S. B. Chowdhury, S. Chakrabarty, T. Chakrabarty, D. C. Mukherjee, *Colloids Surf. A* **1995**, *103*, 59–71; b) C. V. Gherasim, G. Bourceanu, *Chem. Eng. J.* **2013**, *220*, 24–34.

[6] a) J.-R. Li, J. Sculley, H.-C. Zhou, *Chem. Rev.* **2012**, *112*, 869–932; b) L. J. Murray, M. Dinca, J. R. Long, *Chem. Soc. Rev.* **2009**, *38*, 1294–1314; c) M. J. Manos, R. G. Iyer, E. Quarez, J. H. Liao, M. G. Kanatzidis, *Angew. Chem.* **2005**, *117*, 3618–3621; *Angew. Chem. Int. Ed.* **2005**, *44*, 3552–3555; d) S. Das, H. Kim, K. Kim, *J. Am. Chem. Soc.* **2009**, *131*, 3814–3815; e) B. Liu, *J. Mater. Chem.* **2012**, *22*, 10094–10101; f) F. N. Dai, H. Y. He, D. F. Sun, *J. Am. Chem. Soc.* **2008**, *130*, 14064–14065; g) M. Yoon, R. Srirambalaji, K. Kim, *Chem. Rev.* **2012**, *112*, 1196–1231; h) J. Lee, O. K. Farha, J. Roberts, K. A. Scheidt, S. T. Nguyen, J. T. Hupp, *Chem. Lett. Chem. Soc. Rev.* **2009**, *38*, 1450–1459; i) Q. Fang, G. Zhu, Z. Jin, M. Xue, X. Wei, D. Wang, S. Qiu, *Angew. Chem.* **2006**, *118*, 6272–6276; *Angew. Chem. Int. Ed.* **2006**, *45*, 6126–6130; j) Y. Liu, J. F. Eubank, A. J. Cairns, J. Eckert, V. C. Kravtsov, R. Luebke, M. Eddaoudi, *Angew. Chem.* **2007**, *119*, 3342–3347; *Angew. Chem. Int. Ed.* **2007**, *46*, 3278–3283.

[7] a) H. H. Fei, M. R. Bresler, S. R. J. Oliver, *J. Am. Chem. Soc.* **2011**, *133*, 11110–11113; b) P. F. Shi, B. Zhao, G. Xiong, Y. L. Hou, P. Cheng, *Chem. Commun.* **2012**, *48*, 8231–8233; c) H. H. Fei, C. S. Han, J. C. Robins, S. R. J. Oliver, *Chem. Mater.* **2013**, *25*, 647–652; d) R. Custelcean, P. V. Bonnesen, N. C. Duncan, X. H. Zhang, L. A. Watson, G. V. Berkel, W. B. Parson, B. P. Hay, *J. Am. Chem. Soc.* **2012**, *134*, 8525–8534.

[8] a) S. R. J. Oliver, *Chem. Soc. Rev.* **2009**, *38*, 1868–1881; b) S. X. Liu, L. H. Xie, B. Gao, C. D. Zhang, C. Y. Sun, D. H. Li, Z. M. Su, *Chem. Commun.* **2005**, 5023–5025; c) H. H. Fei, D. L. Rogow, S. R. J. Oliver, *J. Am. Chem. Soc.* **2010**, *132*, 7202–7209; d) X. D. Chen, C. Q. Wan, H. H. Y. Sung, I. D. Williams, T. C. W. Mak, *Chem. Eur. J.* **2009**, *15*, 6518–6528; e) G. Nickerl, A. Notzon, M. Heitbaum, I. Senkovska, F. Glorius, S. Kaskel, *Cryst. Growth Des.* **2013**, *13*, 198–203; f) B. Manna, A. K. Chaudhari, B. Joarder, A. Karmakar, S. K. Ghosh, *Angew. Chem.* **2013**, *125*, 1032–1036; *Angew. Chem. Int. Ed.* **2013**, *52*, 998–1002.

[9] D. Liu, H. X. Li, Z. G. Ren, Y. Chen, Y. Zhang, J. P. Lang, *Cryst. Growth Des.* **2009**, *9*, 4562–4566.

[10] a) S. T. Zheng, F. Zuo, T. Wu, B. Irfanoglu, C. Chou, R. A. Nieto, P. Y. Feng, X. H. Bu, *Angew. Chem.* **2011**, *123*, 1889–1892; *Angew. Chem. Int. Ed.* **2011**, *50*, 1849–1852; b) S.-T. Zheng, T. Wu, B. Irfanoglu, F. Zuo, P. Feng, X. Bu, *Angew. Chem.* **2011**, *123*, 8184–8187; *Angew. Chem. Int. Ed.* **2011**, *50*, 8034–8037; c) W. G. Lu, C. Y. Su, T. B. Lu, L. Jiang, J. M. Chen, *J. Am. Chem. Soc.* **2006**, *128*, 34–35; d) Y. Kang, F. Wang, J. Zhang, X. H. Bu, *J. Am. Chem. Soc.* **2012**, *134*, 17881–17884; e) S. T. Zheng, T. Wu, F. Zuo, C. S. Chou, P. Y. Feng, X. H. Bu, *J. Am. Chem. Soc.* **2012**, *134*, 1934–1937; f) X. S. Wang, L. Meng, Q. G. Cheng, C. Kim, L. Wojtas, M. Chrzanowski, Y. S. Chen, X. P. Zhang, S. Q. Mat, *J. Am. Chem. Soc.* **2011**, *133*, 16322–16325.

[11] L. Carlucci, G. Ciani, S. Maggini, D. M. Proserpio, M. Visconti, *Chem. Eur. J.* **2010**, *16*, 12328–12341.

[12] D. T. Tran, P. Y. Zavalij, S. R. J. Oliver, *J. Am. Chem. Soc.* **2002**, *124*, 3966–3969.

[13] a) M. M. Hoffmann, J. G. Darab, J. L. Fulton, *J. Phys. Chem. A* **2001**, *105*, 1772–1782; b) K. Sugawara, M. Akita, M. Akita, *Dalton Trans.* **2003**, 4346–4355.
[14] a) B. C. Tzeng, T. H. Chiu, B. S. Chen, G. H. Lee, *Chem. Eur. J.* **2008**, *14*, 5237–5245; b) J. Fan, L. Gan, H. Kawaguchi, W. Y. Sun, K. B. Yu, W. X. Tang, *Chem. Eur. J.* **2003**, *9*, 3965–3973.
[15] a) X. P. Li, J. Y. Zhang, M. Pan, S. R. Zheng, Y. Liu, C. Y. Su, *Inorg. Chem.* **2007**, *46*, 4617–4625; b) X. H. Jin, J. K. Sun, L. X. Cai, J. Zhang, *Chem. Commun.* **2011**, *47*, 2667–2669.